

## List of Publications (Under the Thesis work)

1.		<p><b>Title: Investigation of Rheological and Thermal Conductivity Properties of Castor Oil Nanofluids Containing Graphene Nanoplatelets.</b></p> <p>Vishal Vora, Rakesh K. Sharma, and D. P. Bharambe  <b>International Journal of Thermophysics (2023) 44:155</b>          Published online: 9 October 2023  <a href="https://doi.org/10.1007/s10765-023-03264-5">https://doi.org/10.1007/s10765-023-03264-5</a></p>
----	---	--

## List of Presentations (Under the Thesis work)

1.		<p><b>Title: Assessment of Rheological behaviour and Thermal conductivity of Nonedible Castor Oil for possible lubrication applications.</b></p> <p>Vishal Vora, Rakesh K. Sharma, and D. P. Bharambe  <b>National Conference on “Modern Trends in Chemistry”</b>, RR Mehta College of Science and CL Parikh College of Commerce, Palanpur.          Date of presentation: 13 March 2022          Presented session: ORAL</p>
2.		<p><b>Title: Investigation of Rheological and Thermal Conductivity Properties of Castor Oil Nanofluids Containing Graphene Nanoplatelets.</b></p> <p>Vishal Vora, Rakesh K. Sharma, and D. P. Bharambe  <b>International Seminar on Advanced Materials and Applications</b>, Applied Physicas Department and Applied Chemistry Department, Faculty of Technology and Engineering, M.S. University of Baroda, Baroda.          Date of presentation: 18 July 2022          Presented session: POSTER</p>



# Investigation of Rheological and Thermal Conductivity Properties of Castor Oil Nanofluids Containing Graphene Nanoplatelets

Vishal Vora<sup>1,2</sup> · Rakesh K. Sharma<sup>1</sup> · D. P. Bharambe<sup>1</sup>

Received: 11 September 2023 / Accepted: 19 September 2023 / Published online: 9 October 2023  
© The Author(s), under exclusive licence to Springer Science+Business Media, LLC, part of Springer Nature 2023

## Abstract

Non-edible oils hold great potential as a viable feedstock for bio-lubricant production. Among these oils, castor oil stands out due to its unique hydroxyl group structure. Castor oil finds applications in various fields such as lubrication, dielectrics, and heat transfer. This study focused on investigating the dynamic viscosity and thermal conductivity of castor oil and graphene nanoplatelets/castor oil nanofluids. The nanofluids were synthesized through a two-step process involving the combination of graphene nanoplatelets crystal powder with pure castor oil. Morphological and crystallographic analyses revealed platelet-shaped graphene nanoplatelets with a prominent (002) reflection. Dynamic viscosity measurements were performed using a rheometer at temperatures ranging from 40 °C to 100 °C, and thermal conductivity assessments were conducted using the Modified Transient Plane Source technique from 30 °C to 70 °C. Investigation revealed that as temperature increased, the nanofluids exhibited a significant decrease in dynamic viscosity. Conversely, the dynamic viscosity increased moderately with higher concentrations of graphene nanoplatelets. Importantly, the addition of graphene nanoplatelets did not disrupt the Newtonian flow behavior of castor oil. Furthermore, the study demonstrated a remarkable enhancement in thermal conductivity with increasing concentrations of graphene nanoplatelets. This enhancement can be attributed to the high conductivity of graphene nanoplatelets. Overall, biodegradable graphene nanoplatelets/castor oil nanofluid present promising prospects as an advanced lubricating oil with superior heat transfer properties. This research contributes to the understanding and utilization of nanofluids for effective thermal management applications.

**Keywords** Castor oil · Dynamic viscosity · Graphenenanoplatelets · Newtonian fluid · Nanofluids · Shear rate

## 1 Introduction

In recent times, worldwide environmental concerns have driven industries to transition toward using bio-based fluids in a range of applications, including lubrication, insulation, and heat transfer. These applications were historically dominated by mineral oils. Vegetable oils, as a sustainable alternative, offer a range of advantageous properties. These oils exhibit excellent lubricity, ensuring smooth operation and reducing friction-related wear and tear. Their high dynamic viscosity index allows them to maintain effective lubrication across different temperature and pressure conditions. Additionally, vegetable oils have high flash points, enhancing safety during storage and handling. They also possess good dielectric properties, making them suitable for electrical insulation applications. Furthermore, their non-toxic nature promotes a safer working environment. These inherent properties of vegetable oils make them a promising choice for replacing mineral oil-based fluids, contributing to a more sustainable and environmentally friendly approach to industrial processes [1, 2]. In response to the specific demands of various industries, there has been a growing interest in enhancing the properties of vegetable oils by incorporating nanoparticles into the base fluid. These fluids, known as nanofluids, consist of nanoparticles with diameters smaller than 100 nm dispersed within the base fluids [3]. Nanomaterials, with their exceptionally large surface area, offer high reactivity compared to their bulk form. The incorporation of nanoparticles into base fluids enhances thermal conductivity, viscosity, and other properties, resulting in bio-based nanofluids with advantages over traditional fluids. These nanofluids improve thermal conductivity, rheology, conductive heat transfer coefficient, analytic heat flux, and wettability, making them popular for enhancing efficiency in heat transfer and lubrication processes. This innovative utilization of nanofluids addresses the industry's evolving needs while prioritizing sustainability and environmental responsibility [4].

Recent advancements in nanofluid research have focused on enhancing thermal conductivity, attracting considerable attention from the scientific community [5]. The prolonged lifespan of lubricating oil is significantly dependent on its efficiency in heat transfer. Thermal conductivity plays a crucial role in maintaining the oil's characteristics and prolonging its operational lifespan [6]. Numerous studies have investigated the addition of highly thermally conductive nanomaterials, such as metal oxides, metal nitrides, pure metals, diamonds, carbon nanotubes, graphene oxide, graphene, and hybrid materials, to base fluids to improve thermal conductivity [7–10]. These nanofluids, characterized by their enhanced thermal conductivity, offer multiple advantages in various heat transfer and lubrication applications. The assessment of viscosity is particularly important in these applications, where nanofluids are pumped through pipes or provide lubrication to moving parts, ensuring compatibility and performance in specific industrial settings [11–14].

Recent literature has witnessed a significant number of research publications focusing on the synthesis of nanofluids using carbon-based nanostructures,

including graphene, graphene oxide, and carbon nanotubes (both single-wall and multiwall) [15–22]. Among these carbon-based nanomaterials, graphene has received special attention due to its exceptional thermal conductivity [23]. Graphene, composed of hexagonally arranged,  $sp^2$ -bonded carbon atoms, is a single-atom-thick sheet [24]. However, producing pure graphene on a large scale remains a commercial challenge. This is due to the high costs involved in manufacturing and separating two-dimensional graphene crystals. Achieving the same quality as seen in research laboratories presents significant difficulties when trying to scale up the process [25]. In contrast, graphene nanoplatelets (GNP) offer advantages such as large-scale production capability, cost-effectiveness, and desirable physical properties. GNP consists of two-dimensional carbon structures with a single or multilayer graphite plane, measuring 5 to 10 nm in overall thickness and ranging in dimensions from 1  $\mu\text{m}$  to 50  $\mu\text{m}$  [26]. GNP possesses exceptional functional properties, including high thermal and electrical conductivity, mechanical toughness, low weight, a high aspect ratio, and a flat structure [27, 28].

Selvam et al. [29] conducted a comprehensive investigation on the thermal conductivity behavior of GNP nanofluids in EG(ethylene glycol) and water base fluids. The nanofluids were prepared by incorporating GNP at volume percentages of 0.001, 0.01, 0.1, 0.2, 0.3, 0.4, and 0.5% in both EG and water, with the addition of 0.75 volume% sodium deoxycholate (as surfactant). The thermal conductivities of the nanofluids were measured at 30 °C using the transient hot wire method. The experimental results demonstrated a notable increase in thermal conductivity as the volume percentage of GNP in the base fluid increased. The highest enhancements in thermal conductivity were observed at 0.5 volume% GNP, with a 21% increase in EG and a 16% increase in water base fluids, respectively. Similarly, Mehrali et al. [6] conducted a study focusing on the rheological properties and thermal conductivity of GNP/water nanofluids. The rheological study of the nanofluids was found to demonstrate both Newtonian and non-Newtonian characteristics, with the dynamic viscosity decreasing linearly with increasing temperature. Moreover, the results revealed that the thermal conductivity of the base fluid increased with the incorporation of GNP, demonstrating the positive influence of GNP on thermal conductivity in the nanofluid system.

In a comprehensive investigation by Cabaleiro et al. [30], the thermal conductivity, dynamic viscosity, and density properties of nanofluids composed of EG and a water mixture as the base fluid were examined. The nanofluids were prepared by dispersing sulfonic acid-functionalized GNP at weight percentages of 0.10, 0.25, and 0.50. The study findings revealed that increasing the weight percentage of sulfonic acid-functionalized GNP in the base fluid led to a notable enhancement in thermal conductivity. This indicates the potential of sulfonic acid-functionalized GNP to improve heat transfer properties within the nanofluid. Furthermore, the addition of sulfonic acid-functionalized GNP resulted in an increase in the dynamic viscosity of the nanofluid, as demonstrated by rheological analysis. However, it is worth noting that temperature had a direct impact on the density and caused changes in the fluid's viscosity without affecting the heat transfer characteristics of the nanofluid. This investigation sheds light on the influence of sulfonic acid-functionalized GNP

on the thermal and rheological properties of nanofluids, providing valuable insights for potential applications in heat transfer systems.

Suhaib et al. [31] conducted research into the rheological behavior of hybrid nanofluids containing diamond-GNP and mineral oil. They studied these nanofluids at different shear rates, ranging from  $1 \text{ s}^{-1}$  to  $2000 \text{ s}^{-1}$ . They prepared hybrid nanofluids with diamond-GNP concentrations varying from 0.0 wt to 2.0 wt for the investigation. The findings showed that adding 2% diamond-GNP increased the dynamic viscosity of the hybrid nanofluid by 35%. The rheological properties indicated that the mineral oil-based hybrid nanofluid exhibited shear-thinning non-Newtonian behavior. This behavior was analysed using the Ostwald-de-Waele (OdW) model.

In another study by Muthuraj et al. [32], the impact of GNP on the thermal conductivity of sunflower oil was investigated. The thermal conductivities of nanofluids containing GNP concentrations ranging from 0.1 wt% to 0.5 wt% in sunflower oil were measured using the transient hot wire technique within a temperature range of  $40 \text{ }^{\circ}\text{C}$  to  $100 \text{ }^{\circ}\text{C}$ . The findings demonstrated that the thermal conductivity increased with the concentration of GNP. Furthermore, it was observed that the thermal conductivity was lower at lower temperatures. Specifically, maximum enhancements in thermal conductivity were achieved at GNP concentrations of 5.7%, 6.8%, and 8.1% for GNP concentrations of 0.1%, 0.3%, and 0.5%, respectively.

Fidan-Aslan et al. [33] investigated the preparation and characterization of GNP nanofluids using PEG-POSS (polyethylene glycol derived polyhedral oligomeric silsesquioxane) as a stabilizer. Ultrasound-assisted methods were employed to prepare nanofluids at high GNP concentrations in water and EG. The addition of PEG-POSS demonstrated a reduction of surface tension by 4.5% for water-based nanofluids, while EG-based nanofluids showed an increase of almost 11.5%. The thermal conductivity increment of 32% was achieved in EG-based 2.0 wt% GNP nanofluids. This research provides valuable insights for the development of heat transfer systems requiring improved thermal conductivity and appropriate rheological behavior.

The literature mentioned above emphasizes the favourable outcomes of adding graphene nanoplatelets (GNP) to different base fluids and oils. Incorporating GNP leads to improvements in both conductivity and viscosity. However, there is currently a lack of studies on the rheology and thermal conductivity of GNP/castor oil (CO) nanofluids. Castor oil is derived from the seeds of the *Ricinus communis* L. plant, which is predominantly cultivated in India, South America, and Africa [34]. What sets castor oil apart from other vegetable oils is its unique hydroxyl ( $-\text{OH}$ ) group structure. It is a triglyceride that consists solely of ricinoleic acid, an 18-carbon monounsaturated fatty acid with a hydroxyl group at the 12<sup>th</sup> carbon [35]. Moreover, castor oil falls under the category of non-edible oils among vegetable oils. Non-edible plant oils hold significant promise as resources for the production of bio-lubricants. They offer cost advantages over edible oils, as the latter are primarily used for human food consumption. In developing countries, non-edible oil-based lubricants present a promising alternative to mineral-based lubricating oils. Non-edible oil plants are abundantly available in large quantities worldwide [36].

Previous studies have investigated the use of castor oil (CO) in combination with various nanofriction modifiers such as zinc oxide [37], molybdenum disulfide ( $\text{MoS}_2$ ) [38], hexagonal boron nitride [39], copper oxide (CuO) nanoparticles [40],

as well as nanocelluloses or nanoclays [41] as electro-sensitive lubricants. These investigations have highlighted the potential of CO-based nanolubricants in different applications. However, the rheological and thermal properties of GNP dispersed in CO nanofluids have not been explored. The unexplored GNP/CO nanofluid holds significant potential as a novel non-edible vegetable oil-based lubricating oil, heat transfer fluid, and/or dielectric fluid in various industrial applications. Understanding the rheological behavior and thermal characteristics of this nanofluid system can provide valuable insights into its suitability and performance in different operational conditions. Further investigation into the GNP/CO nanofluid can pave the way for its potential applications as an advanced lubricant, efficient heat transfer medium, and reliable dielectric fluid in diverse industrial settings.

In this study, we investigated the rheological behavior of graphene nanoplatelets (GNP) dispersed in castor oil (CO) nanofluids under various conditions. The analysis was conducted over a temperature range of 40 °C to 100 °C, with different GNP concentrations ranging from 0.05 to 0.5 weight% and varying shear rates from 10 s<sup>-1</sup> to 150 s<sup>-1</sup>. The changes in the dynamic viscosity of the nanofluid were examined considering the temperature, GNP concentration, and shear rate parameters. The fluid behavior was characterized using the OdW model, enabling the evaluation of the power law index (n) and consistency index (m). Furthermore, the thermal conductivity of the GNP/CO nanofluids was measured within the temperature range of 40 °C to 100 °C. The thermal conductivity of the nanofluid to the base fluid ratio was calculated, providing insights into the thermal conductivity enhancement conferred by the incorporation of GNP. This investigation contributes to a comprehensive understanding of the rheological properties and thermal conductivity behavior of GNP/CO nanofluids, enabling their potential applications as advanced lubricants, efficient heat transfer fluids, and reliable dielectric fluids in various industrial scenarios.

## 2 Experimental Section

### 2.1 Preparation of GNP/CO nanofluids

The preparation of nanofluids involves careful attention to achieve a stable liquid suspension without aggregation or deposition over an extended period. Figure 1 presents the actual image of graphene nanoplatelets (GNP) dispersed in castor oil (CO). The GNP, with a thickness of 6 to 8 nm and a width of 25 μm, was procured from Tokyo Chemical Industry (TCI), Japan.

The CO was obtained from Loba-Chemie, India, and its chemical and physical properties are provided in Table 1, as specified in the certificate of analysis.

The process to create the nanofluids involved two steps. First, a precise amount of GNP was weighed using a highly accurate analytical balance (Mettler Toledo XSR105) with a precision of ±0.02 mg. This was done to achieve GNP weight percentages of 0.05, 0.1, 0.2, and 0.5 in the corresponding weight of CO. Following this, the GNP and CO mixtures were subjected to ultrasonication using a high-powered ultrasonic probe (Leela Sonic) with a 3 mm diameter. The ultrasonication was

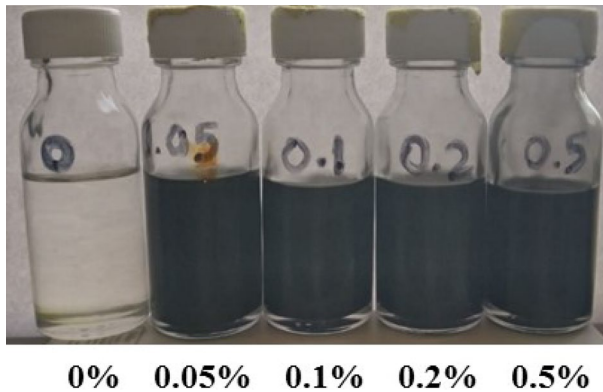


**Fig. 1** Photograph of pure CO and GNP/CO nanofluids

**Table 1** Properties of CO

Property	Value
Appearance	Yellow colored viscous liquid
Specific gravity (at 25°C)	0.960
Hydroxyl number	162
Saponification value	178.18
Iodine number	83.11
Acid value (mg KOH/gm of oil)	0.15

performed at a frequency of 20 kHz and an output power of 500 watts. This process continued for 3 h in pulse mode of 2 s ON and 2 s OFF at a controlled temperature of 40 °C to 50 °C [42, 43]. Through this ultrasonication, stable and uniform GNP/CO nanofluids were formed. It's important to note that the presence of a ricinoleic acid ester in CO itself acted as a surfactant, further enhancing the stability of the nanodispersion. The prepared GNP/CO nanofluids were subjected to rheological and thermal analysis immediately, within a three-day time frame.

## 2.2 Characterization of GNP

The morphology of GNP was examined using Scanning Electron Microscopy (SEM) with a JEOL JSM-6380LV instrument, as depicted in Fig. 2a and b. The SEM images reveal that the GNP nanoparticles possess a distinctive platelet shape.

The X-ray diffraction (XRD) analysis of GNP was performed using a D8-advance diffractometer with Cu-K $\alpha$  X-ray radiation (Bruker). The XRD measurements were conducted at a scan rate of 1°min<sup>-1</sup> over a 2 $\theta$  range of 3° to 60°. The results of the XRD analysis for GNP are presented in Fig. 3. The XRD pattern exhibits characteristic peaks indicating the graphite-like nature of GNP. Notably, sharp reflections at

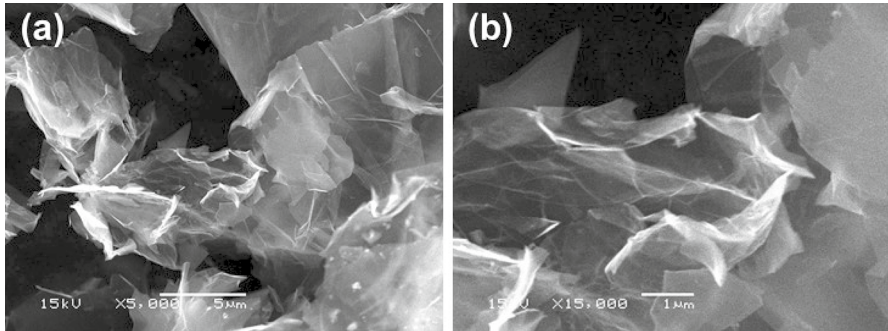


**Fig. 2** (a) and (b) SEM pictures of GNP

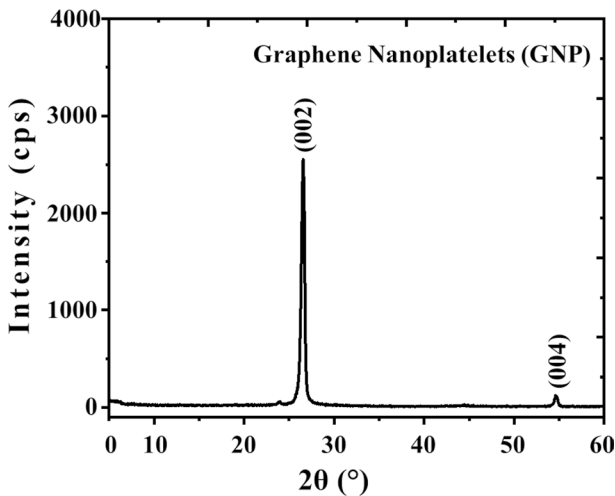


**Fig. 3** XRD pattern of GNP

$2\theta=26.6^\circ$  corresponding to the (002) plane and at  $2\theta=54.7^\circ$  corresponding to the (004) plane were observed. These sharp reflections are indicative of the high crystallinity of GNP.

### 2.3 Methodology (Experimental)

The shear dynamic viscosity of the GNP/CO oil nanofluids was assessed using a rotational rheometer (HAAKE MARS, Thermo Scientific), as shown in Fig. 4a. This rheometer is equipped with parallel plates geometry (P25 CS L) for conducting rheological studies. A peltier temperature measuring system allows tests to be conducted at a consistent temperature ranging from 40 °C to 100 °C, with an accuracy of  $\pm 0.1$  °C. The nanofluids were placed between the parallel plates and left for 15 min to ensure temperature stability. The rheological data were input into



**Fig. 4** (a) Rotational rheometer and (b) thermal conductivity meter

computer-controlled RheoWin software provided by Thermo Scientific. This software was used for conducting scans between temperature 40 °C and 100 °C while maintaining a dynamic shear rate ranging from 10 s<sup>-1</sup> to 150 s<sup>-1</sup> at intervals. Each experimental value was an average of 20 readings taken for each experiment.

Thermal conductivity measurements were conducted using a thermal conductivity analyzer (Trident, C-Therm Technologies) employing the Modified Transient Plane Source (MTPS) technique. This method is versatile and allows the analysis of the thermal properties of solid materials, fluids, and amorphous powders. The measurement setup, depicted in Fig. 4b, includes an MTPS sensor, control electronics, an oven, and dedicated computer software. For each measurement, approximately 1 mL to 2 mL of the nanofluid sample was introduced into the sensor module, which was then positioned within an oven. The thermal conductivity of the nanofluid was examined within the temperature range of 30°C to 70 °C with an accuracy of  $\pm 0.1$  °C. Each experimental value was an average of 10 readings taken for each experiment. As per the manufacturer's procedure to ensure the sensor's performance, the thermal conductivity of ultrapure water (0.6090 W/(mK)) was measured before each nanofluid measurement [44].

The uncertainty for measuring dynamic viscosity and thermal conductivity is  $\pm 3.8\%$ , and  $\pm 5.0\%$ , respectively.

The use of the rotational rheometer and the MTPS technique allows for precise viscosity and thermal conductivity measurements, respectively, providing valuable insights into the rheological and thermal properties of the GNP/CO nanofluids.

### 3 Results and Discussion

In this study, a comprehensive rheological investigation was conducted to evaluate the dynamic viscosity of both pure castor oil (CO) and GNP/CO nanofluids under different GNP concentrations, shear rates, and temperature conditions. The main focus was to understand the influence of GNP weight percentage and temperature on the dynamic viscosity and thermal conductivity of GNP/CO nanofluids. The obtained results shed light on the potential applications of GNP/CO nanofluids as lubricating oils.

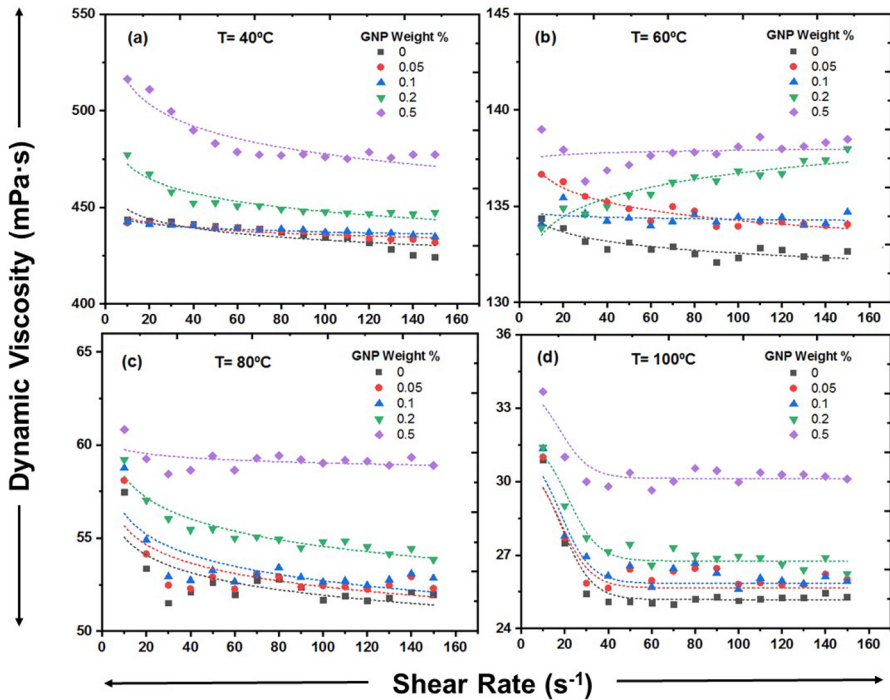


**Fig. 5** (a) and (d) Effect of shear rate on dynamic viscosity of GNP/CO nanofluids at different mass fraction

Figure 5 exhibits the impact of shear rate on the dynamic viscosity of GNP/CO nanofluids at different GNP weight percentages and temperatures ranging from 40 °C to 100 °C. The results indicate that the dynamic viscosity of both GNP/CO nanofluids and pure CO decreases non-linearly at lower shear rates (up to 40  $s^{-1}$ ) for all temperatures. At higher shear rates, all fluids exhibit linear behavior. The experimental findings suggest a newtonian fluid behavior for both GNP/CO nanofluids and pure CO at higher shear rates within the experimental range. Furthermore, at higher shear rates, nanofluids with higher GNP weight percentages exhibit a slight shear-thinning behavior compared to nanofluids with lower GNP weight percentages. This observation suggests that increased GNP concentration, represented by weight percentage, has a notable impact on enhancing shear thinning in both GNP/CO nanofluids and pure CO.

Figure 6 presents the impact of GNP weight percentage on the dynamic viscosity of nanofluids at a constant temperature. The GNP concentration has a significant influence on the dynamic viscosity within the shear rate range of 10  $s^{-1}$  to 150  $s^{-1}$ . At a fixed shear rate of 150  $s^{-1}$  and a temperature of 40 °C, the nanofluid viscosities are 424.4 mPa·s and 477.3 mPa·s for GNP concentrations of 0.0 wt% and 0.5 wt%, respectively (Fig. 6a). When the shear rate decreases from 150  $s^{-1}$  to 10  $s^{-1}$ , the nanofluid viscosities increase to 443.7 mPa·s and 516.4 mPa·s for GNP concentrations of 0.0 and 0.5 weight%, respectively. This is attributed to the

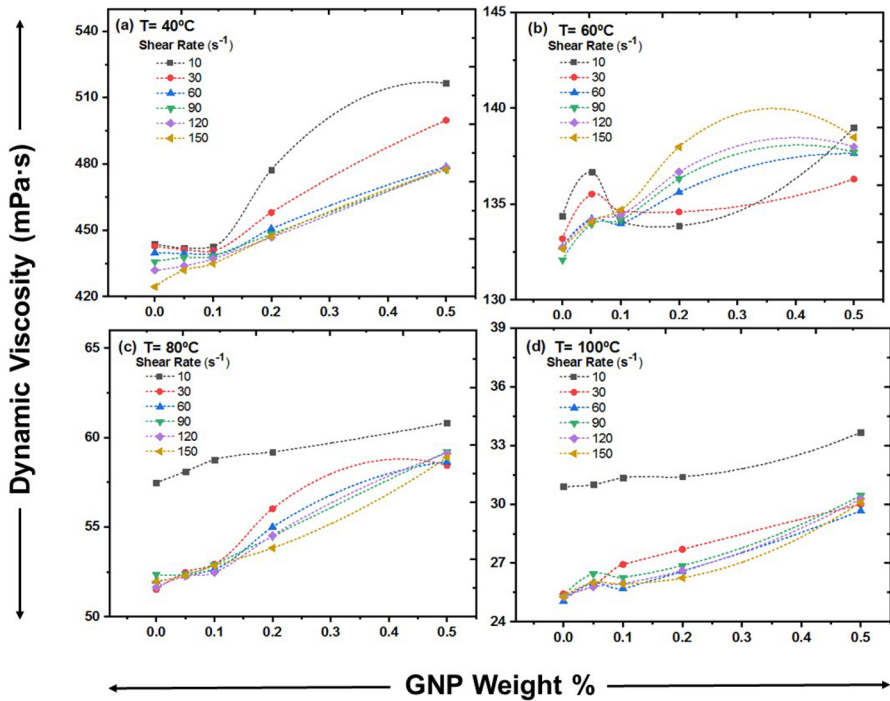


Fig. 6 (a) and (d) Effect of solid mass fractions on dynamic viscosity of GNP/CO nanofluids at different shear rates

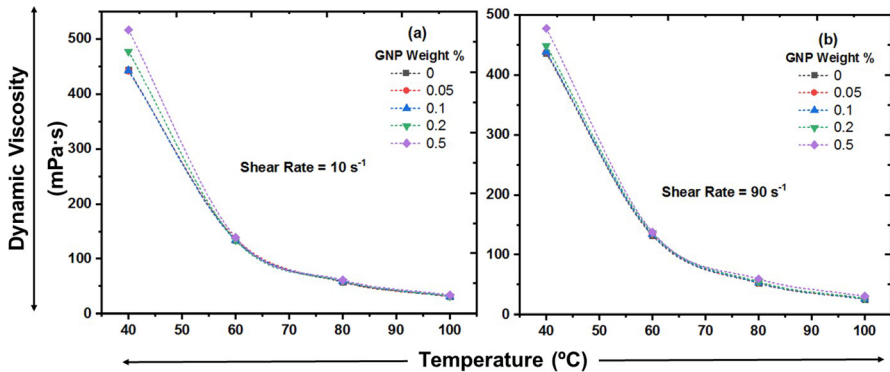


Fig. 7 (a) and (b) Effect of temperature on the dynamic viscosity of GNP/CO nanofluids at different solid mass fractions

enhanced resistance to flow depicted by the presence of solid nanoparticles in the CO fluid [1]. Consequently, increasing the GNP concentration results in higher nanofluid viscosity. However, it is worth noting that the dynamic viscosity does not always increase significantly with concentration. For instance, in Fig. 6c and

d, the increase in dynamic viscosity at  $10 \text{ s}^{-1}$  is relatively low compared to higher shear rates.

Figure 7 depicts the influence of temperature on the dynamic viscosity of pure castor oil (CO) as well as GNP/CO nanofluids with varying GNP weight percentages. This analysis is conducted at constant shear rates of  $10 \text{ s}^{-1}$  and  $150 \text{ s}^{-1}$ . As the temperature rises from  $40 \text{ }^\circ\text{C}$  to  $100 \text{ }^\circ\text{C}$ , the dynamic viscosity decreases for both CO fluids and GNP/CO nanofluids. For instance, at a shear rate of  $10 \text{ s}^{-1}$ , the GNP/CO nanofluid with a 0.5 wt% GNP concentration shows a viscosity of 516.4 mPa at  $40 \text{ }^\circ\text{C}$ , which decreases to 33.7 mPa at  $100 \text{ }^\circ\text{C}$ . Similar trends are observed for other GNP weight percentages. These observations can be attributed to a decrease in intermolecular adhesion forces as temperature rises. Moreover, the effect of solid GNP concentration on dynamic viscosity is more prominent at lower temperatures. However, this influence becomes less significant as the temperature increases. This trend is illustrated in Fig. 7a and b.

In Fig. 8a–d, the relationship between shear stress and shear rate of GNP/CO nanofluid is depicted at different temperatures for various GNP weight percentages (0.0, 0.05, 0.1, 0.2, and 0.5). The figures demonstrate that shear stress increases as shear rate increases across all temperatures. To determine the flow behavior of the fluid, whether it follows newtonian flow or non-newtonian flow, the Ostwald-de-Waele (OdW) model [7, 45] is employed using Eq. 1:

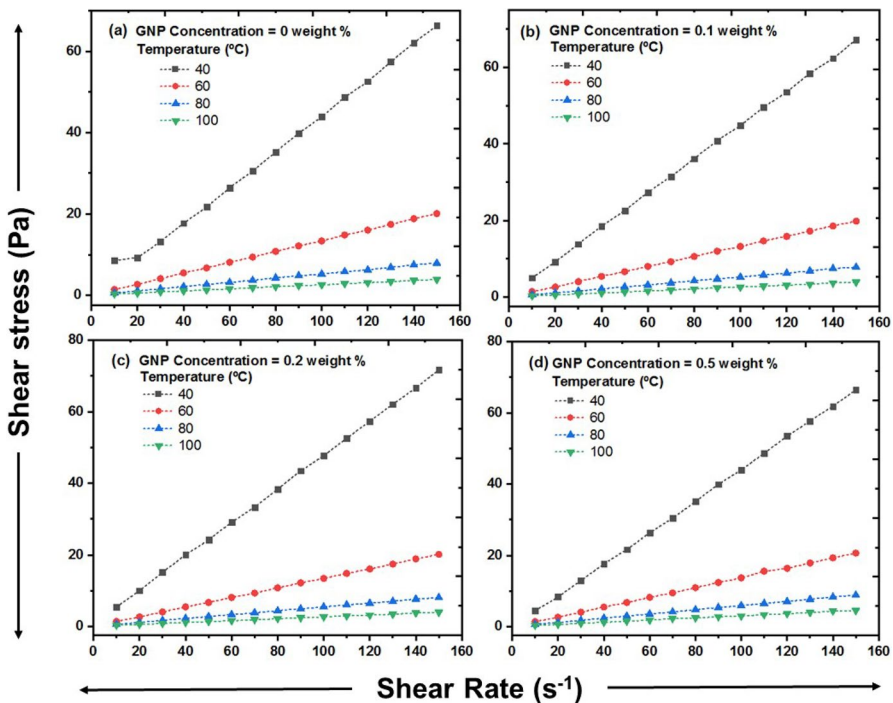
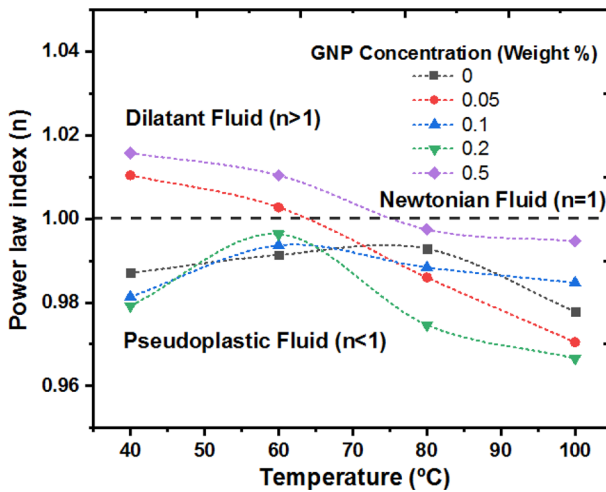


Fig. 8 (a) and (d) Shear stress against shear rate at various temperature for GNP/CO nanofluids

**Table 2** The Power law index (n) and Consistency index (m) values of fluids

GNP concentra- tion (wt%)	Indexes	Temperature (°C)			
		40	60	80	100
0	m	469	140	55	29
	n	0.987	0.991	0.993	0.978
0.05	m	420	137	56	29
	n	1.010	1.003	0.986	0.970
0.1	m	490	137	56	28
	n	0.981	0.994	0.988	0.985
0.2	m	528	137	62	31
	n	0.979	0.996	0.975	0.967
0.5	m	410	131	60	31
	n	1.016	1.010	0.997	0.995



**Fig. 9** Power law index for different solid mass fractions and temperature for GNP/CO nanofluids

$$\tau = m \cdot \gamma^n \tag{1}$$

where,  $\tau$  is shear stress,  $\gamma$  is shear rate,  $m$  is the consistency index, and  $n$  is the power law index.

In Eq. 1, the power law index ( $n$ ) characterizes the rheological aspects of fluids, while the consistency index ( $m$ ) describes the fluid’s flow resistance. Fluids can be classified into three types based on the value of  $n$ : Newtonian behavior ( $n=1$ ), non-newtonian dilatant behavior ( $n>1$ ), and non-newtonian pseudoplastic behavior ( $n<1$ ). In this analysis, a power law curve fitting was applied to the shear stress against shear rate curve (Fig. 8) to determine the values of  $m$  and  $n$ . The obtained values of  $m$  and  $n$  are presented in Table 2.

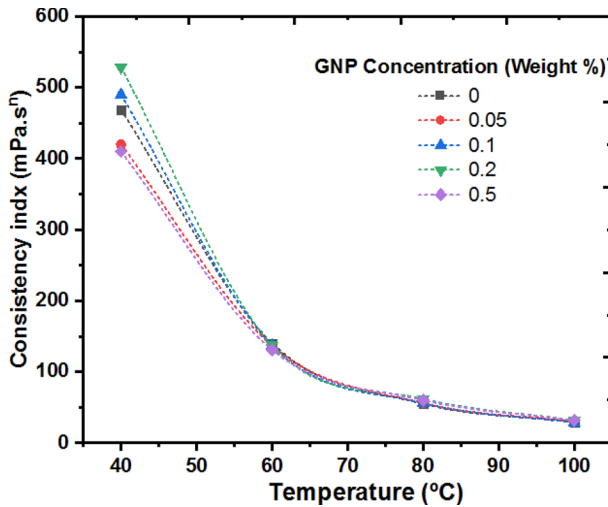


Fig. 10 Consistency index for different solid mass fractions and temperatures for GNP/CO nanofluids

As shown in Fig. 9, the values of  $n$  for all GNP weight percentages and temperature ranges of the nanofluids are close to or equal to one, indicating a Newtonian flow behavior.

Furthermore, Fig. 10 depicts the relationship between the temperature of the nanofluids and the consistency index ( $m$ ) for different GNP weight concentrations. The results clearly demonstrate a decrease in the value of  $m$  with increasing temperature. This indicates that as the temperature rises, the fluid's mobility decreases, resulting in reduced resistance to flow.

It is noteworthy that the consistency index does not significantly vary with the GNP concentration at higher temperatures. This observation confirms that higher GNP concentrations in the base fluid do not substantially increase resistance to fluid flow and do not alter the Newtonian behavior of the nanofluids.

In Fig. 11, the thermal conductivity of pure castor oil (CO) and GNP/CO nanofluid is shown as a function of GNP concentration over a temperature range of 30 °C to 70 °C. The results indicate that the thermal conductivity increases with an increase in the GNP concentration. Moreover, at higher GNP concentrations, the thermal conductivity exhibits a steeper slope, indicating a more pronounced enhancement. This increase in thermal conductivity is attributed to the high thermal conductivity of GNP incorporated into the CO fluid. It is noteworthy to notice that the thermal conductivity of both CO fluid and the GNP/CO nanofluid with a 0.05 wt% GNP concentration decreases as the temperature increases. However, a reversal in thermal conductivity behavior is observed at a GNP concentration of 0.5 wt% in the base fluid. In this case, the thermal conductivity of GNP/CO nanofluids increases with increasing temperature. This is explained by the increased interaction and spread of GNP within the CO fluid at higher temperatures. These changes are driven by the energy transfer between the layers of the nanofluid, resulting in improved heat transfer capabilities of the nanofluids.

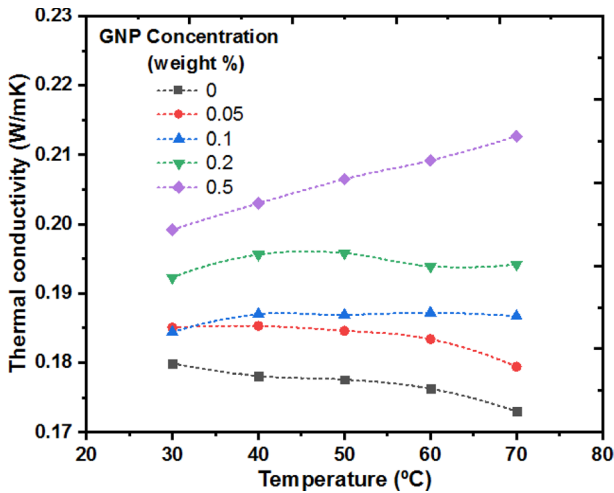


Fig. 11 Thermal conductivity of GNP/CO nanofluids

Overall, the results demonstrate that GNP/CO nanofluids have enhanced thermal conductivity compared to the pure CO fluid.

Equation (2) allows us to calculate the ratio of the thermal conductivity of GNP/CO nanofluid to that of the CO fluid. The equation is given as follows:

$$\text{Thermal conductivity ratio(\%)} = \frac{k(\text{nf})}{k(\text{bf})} \quad (2)$$

where  $k(\text{nf})$  represents the thermal conductivity of nanofluid and  $k(\text{bf})$  acts the thermal conductivity of base fluid.

The thermal conductivity ratio of the GNP/CO nanofluid compared to the CO base fluid is shown in Fig. 12. The ratio increases with increasing temperature. At low GNP weight percentages, there are minimal increases in thermal conductivity due to the lower concentration of GNP in the fluid. However, as the GNP concentration increases, the number of nanoparticles and collisions also increases, resulting in enhanced heat transfer between the fluid layers. This leads to significantly higher thermal conductivity values for the GNP/CO nanofluid compared to the base CO fluid. In our study, the thermal conductivity of the GNP/CO nanofluid increased by 23% at 70 °C for a GNP weight percentage of 0.5%. This significant enhancement demonstrates the potential of GNP/CO nanofluids for improving heat transfer performance in various applications.

## 4 Conclusions

The present study investigates the stability and flow behavior of GNP/CO nanofluids with different GNP concentrations. Through an innovative ultrasonically-assisted technique, the GNP/CO nanofluids were successfully stabilized.

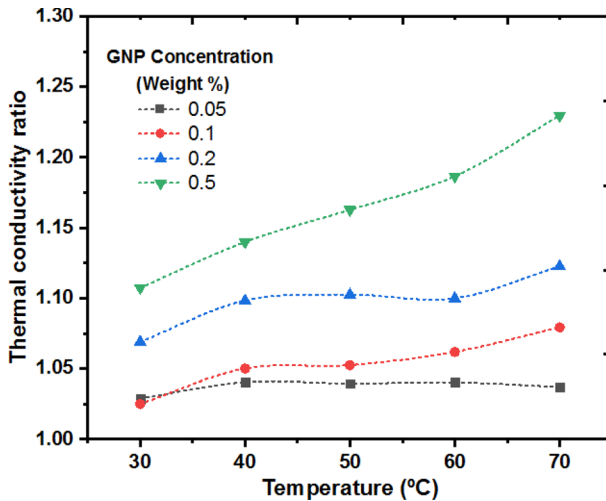


Fig. 12 Thermal conductivity ratio of GNP/CO nanofluids

Rheological investigations were carried out at various shear rates and temperatures, revealing a consistent Newtonian flow behavior across all samples. The study contributes to the existing knowledge on thermophysical properties and sets the stage for further advancements in the field.

The dynamic viscosity of both the CO fluid and GNP/CO nanofluid exhibited a reduction at the initial increase in shear rate of  $20 \text{ s}^{-1}$ . Furthermore, the viscosity remained stable as the shear rate was further increased across all temperatures studied.

The concentration of GNP significantly influences the dynamic viscosity and thermal conductivity behavior of GNP/CO nanofluids. The interactions between GNP and CO play a crucial role in enhancing the heat conduction and transfer capabilities of GNP/CO nanofluids compared to the base CO fluid. In fact, the thermal conductivity was observed to increase by 23% in the best-case scenario at  $70 \text{ }^\circ\text{C}$  for a GNP/CO nanofluid with a weight percentage of 0.5%.

The increased concentration of GNP in the base fluid does not lead to an increase in its dynamic viscosity. This characteristic is advantageous for the application of GNP/CO nanofluids in solar heat collectors where efficient pumping is required.

With increasing temperature from  $40 \text{ }^\circ\text{C}$  to  $100 \text{ }^\circ\text{C}$ , the dynamic viscosity of nanofluids decreases across all GNP concentrations. At lower temperatures of  $40 \text{ }^\circ\text{C}$ , the GNP wt% has a significant impact on viscosity, while its influence diminishes as the temperature rises.

The power law index ( $n$ ) values for all GNP/CO nanofluids, obtained at different temperature ranges, are close to or equal to one. This observation confirms the Newtonian flow behavior of nanofluids.

In conclusion, our study findings strongly suggest that GNP/CO nanofluids hold substantial promise as valuable and cost-effective materials for heat transfer applications. However, we recognize the need for further exploration and meticulous calculations of heat transfer coefficients in practical heat transfer contexts. This approach will provide a comprehensive evaluation of their real-world efficacy.

**Acknowledgments** The corresponding authors acknowledged the CoE of Polymers, Applied Chemistry Department, Faculty of Technology and Engineering for required lab facilities and the Electrical Research and Development Association (ERDA), Vadodara, Gujarat, for kind permission and support in the present research.

**Author Contributions** VV, RKS, DPB contributed equally in preparing and reviewing this manuscript.

**Funding** This work is not supported by other funding.

## Declarations

**Conflict of interest** The authors declare no competing interests.

## References

1. M.N. Rashin, J. Hemalatha, *Exp. Therm. Fluid Sci.* **48**, 67 (2013). <https://doi.org/10.1016/j.expthermflusci.2012.07.019>
2. Z. Shen, F. Wang, Z. Wang, J. Li, *Renew. Sustain. Energy Rev.* **141**, 110783 (2021). <https://doi.org/10.1016/j.rser.2021.110783>
3. S.U. Choi and J.A. Eastman, Argonne National Lab. (ANL), Argonne, IL (United States), Report No. ANL/MSD/CP-84938; CONF-951135–29 (1995).
4. P. Krajnik, F. Pusavec, and A. Rashid, in *Advances in Sustainable Manufacturing: Proceedings of the 8th Global Conference on Sustainable Manufacturing*, Springer Berlin Heidelberg, 107–113 (2011). [https://doi.org/10.1007/978-3-642-20183-7\\_16](https://doi.org/10.1007/978-3-642-20183-7_16)
5. M. Mehrali, S.T. Latibari, M. Mehrali, T.M.I. Mahlia, H.S.C. Metselaar, *Energy* **58**, 628 (2013). <https://doi.org/10.1016/j.energy.2013.05.050>
6. M. Mehrali, E. Sadeghinezhad, S.T. Latibari, S.N. Kazi, M. Mehrali, M.N.B.M. Zubir, and H.S.C. Metselaar, *Nanoscale Res. Lett.* **9**, 1 (2014). <https://doi.org/10.1186/1556-276X-9-15>
7. B.K. Bharath, V.A. MozhiSelvan, *Int. J. Thermophys.* **42**, 37 (2021). <https://doi.org/10.1007/s10765-020-02784-8>
8. N.S. Mane, V. Hemadri, *Int. J. Thermophys.* **43**, 7 (2022). <https://doi.org/10.1007/s10765-021-02938-2>
9. G.A. Longo, C. Zilio, *Int. J. Thermophys.* **34**, 1288–1307 (2013). <https://doi.org/10.1007/s10765-013-1478-z>
10. F.E.B. Bioucas, C. Köhn, A. Jean-Fulcrand et al., *Int. J. Thermophys.* **43**, 167 (2022). <https://doi.org/10.1007/s10765-022-03084-z>
11. J.A. Eastman, S.R. Phillipot, S.U.S. Choi, and P. Keblinski, *Annu. Rev. Mater. Res.* **34**, 219 (2004). <https://doi.org/10.1146/annurev.matsci.34.052803.090621>
12. P. Keblinski, J.A. Eastman, D.G. Cahill, *Mater. Today* **8**, 36 (2005). [https://doi.org/10.1016/S1369-7021\(05\)70936-6](https://doi.org/10.1016/S1369-7021(05)70936-6)
13. I.M. Mahbulul, R. Saidur, M.A. Amalina, *Int. J. Heat Mass Transfer* **55**, 874 (2012). <https://doi.org/10.1016/j.ijheatmasstransfer.2011.10.021>
14. S.V. Sujith, A.K. Solanki, R.S. Mulik, *J. Mol. Liquids* **286**, 110905 (2019). <https://doi.org/10.1016/j.molliq.2019.110905>
15. A. Nasiri, M. Shariaty-Niasar, A.M. Rashidi, R. Khodafarin, *Int. J. Heat Mass Transfer* **55**, 1529 (2012). <https://doi.org/10.1016/j.ijheatmasstransfer.2011.11.004>
16. T.Y. Choi, M.H. Maneshian, B. Kang, W.S. Chang, C.S. Han, D. Poulikakos, *Nanotechnology* **20**, 315706 (2009). <https://doi.org/10.1088/0957-4484/20/31/315706>
17. B. Wright, D. Thomas, H. Hong, L. Groven, J. Puszynski, E. Duke, et al., *Appl. Phys. Lett.* **91**, 173116 (2007). <https://doi.org/10.1063/1.2801507>
18. C. Du et al., *Mathematical Methods in the Applied Sciences* (2020). <https://doi.org/10.1002/mma.6466>

19. L. Chen, H. Xie, *Colloids Surf A Physicochem Eng Asp* **352**, 136–140 (2009). <https://doi.org/10.1016/j.colsurfa.2009.10.015>
20. M.R. Esfahani, E.M. Languri, M.R. Nunna, *Int. Commun. Heat Mass Transf.* **76**, 308–315 (2016). <https://doi.org/10.1016/j.icheatmasstransfer.2016.06.006>
21. M. Kole and T.K. Dey, *J. Appl. Phys.* **113**, 084307 (2013). <https://doi.org/10.1063/1.4793581>
22. S. Almurtaji, N. Ali, J.A. Teixeira et al., *Int. J. Thermophys.* **42**, 168 (2021). <https://doi.org/10.1007/s10765-021-02916-8>
23. A.A. Minea, L. Zupcu, *Int. J. Thermophys.* **43**, 161 (2022). <https://doi.org/10.1007/s10765-022-03093-y>
24. W. Yu, H. Xie, X. Wang, X. Wang, *Phys. Lett. A* **375**, 1323–1328 (2011). <https://doi.org/10.1016/j.physleta.2011.01.040>
25. K.S. Novoselov, V.I. Fal'ko, L. Colombo, P.R. Gellert, M.G. Schwab, and K. Kim, *Nature* **490**, 192–200 (2012). <https://doi.org/10.1038/nature11458>
26. M. Mehrali, S.T. Latibari, M. Mehrali, H.S.C. Metselaar, M. Silakhori, *Energy Convers. Manag.* **67**, 275–282 (2013). <https://doi.org/10.1016/j.enconman.2012.11.023>
27. D.D.L. Chung, *J. Mater. Sci.* **51**, 554–568 (2016). <https://doi.org/10.1007/s10853-015-9284-6>
28. S.Y. Yang, W.N. Lin, Y.L. Huang, H.W. Tien, J.Y. Wang, C.C.M. Ma et al., *Carbon* **49**, 793–803 (2011). <https://doi.org/10.1016/j.carbon.2010.10.014>
29. C. Selvam, D.M. Lal, S. Harish, *Thermochim. Acta* **642**, 32–38 (2016). <https://doi.org/10.1016/j.tca.2016.09.002>
30. D. CabaleiroÁlvarez, L. Colla, S. Barison, L. Lugo Latas, L. Fedele, and S. Bobbo, *Nanoscale Res. Lett.* (2017). <http://hdl.handle.net/11093/3244>
31. S.U. Ilyas, S. Ridha, S. Sardar, P. Estellé, A. Kumar, R. Pendyala, *J. Mol. Liq.* **328**, 115509 (2021). <https://doi.org/10.1016/j.molliq.2021.115509>
32. M. Muthuraj, J. Bensam Raj, and J. Sunil, *Int. J. Nanosci.* **19**, 1950011 (2020). <https://doi.org/10.1142/S0219581X1950011X>
33. T. Fidan-Aslan, E. Alyamac-Seydibeyoglu, *Int. J. Thermophys.* **43**, 75 (2022). <https://doi.org/10.1007/s10765-022-03002-3>
34. V.R. Patel, G.G. Dumancas, L.C.K. Viswanath, R. Maples, and B.J.J. Subong, *Lipid Insights* **9**, LPI-S40233 (2016). <https://doi.org/10.4137/LPI.S40233>
35. A. Hejna, *J. Polym. Sci. Eng.* **1**(3) (2018). <https://doi.org/10.24294/jpse.v1i3.648>
36. M. Balat, *Energy Convers. Manage.* **52**, 1479–1492 (2011). <https://doi.org/10.1016/j.enconman.2010.10.011>
37. S. Bhaumik, R. Maggirwar, S. Datta, S.D. Pathak, *Appl. Surf. Sci.* **449**, 277–286 (2018). <https://doi.org/10.1016/j.apsusc.2017.12.131>
38. K.M.B. Karthikeyan, J. Vijayanand, K. Arun, V.S. Rao, *Mater. Today: Proc.* **39**, 285–291 (2021). <https://doi.org/10.1016/j.matpr.2020.07.128>
39. Y. Wang, Z. Wan, L. Lu, Z. Zhang, Y. Tang, *Tribol. Int.* **124**, 10–22 (2018). <https://doi.org/10.1016/j.triboint.2018.03.035>
40. A.A.S. Noori, H.A. Hussein, and N.S. Namer, *IOP Conf. Ser.: Mater. Sci. Eng.* **518**, 032040 (2019). <https://doi.org/10.1088/1757-899X/518/3/032040>
41. M. García-Morales, S. D. Fernández-Silva, C. Roman, M. A. Olariu, M. T. Cidade, and M. A. Delgado, *Processes* **8**, 1060 (2020). <https://doi.org/10.3390/pr8091060>
42. B. Ruan, A.M. Jacobi, *Nanoscale Res. Lett.* **7**, 1 (2012). <https://doi.org/10.1186/1556-276X-7-127>
43. I.M. Mahbubul, R. Saidur, M.A. Amalina and M.E. Niza, *Int. Commun. Heat Mass Transfer* **76**, 33 (2016). <https://doi.org/10.1016/j.icheatmasstransfer.2016.05.014>
44. M. Iqbal, K. Kouloulias, A. Sergis, and Y. Hardalupas, *J. Therm. Anal. Calorim.* **1–29** (2023) <https://doi.org/10.1007/s10973-023-12334-7>
45. M. Afrand, D. Toghraie, B. Ruhani, *Exp. Thermal Fluid Sci.* **77**, 38 (2016). <https://doi.org/10.1016/j.expthermflusci.2016.04.007>

**Publisher's Note** Springer Nature remains neutral with regard to jurisdictional claims in published maps and institutional affiliations.

Springer Nature or its licensor (e.g. a society or other partner) holds exclusive rights to this article under a publishing agreement with the author(s) or other rightsholder(s); author self-archiving of the accepted manuscript version of this article is solely governed by the terms of such publishing agreement and applicable law.

## Authors and Affiliations

Vishal Vora<sup>1,2</sup> · Rakesh K. Sharma<sup>1</sup> · D. P. Bharambe<sup>1</sup>

✉ Rakesh K. Sharma  
rksharma-appchem@msubaroda.ac.in

✉ D. P. Bharambe  
dpbharambe-appchem@msubaroda.ac.in

<sup>1</sup> Applied Chemistry Department, Faculty of Technology and Engineering, The Maharaja Sayajirao University of Baroda, Vadodara, Gujarat, India

<sup>2</sup> Electrical Research and Development Association, Vadodara, Gujarat, India

## List of Abbreviation

AFA	: Anti-foaming agent
API	: American petroleum institute
ASTM	: American Society for Testing and Materials
AO	: Anti-oxidants
AW	: Anti-wear
BO	: Base oil
BN	: Boron nitride
CO	: Castor oil
CNTs	: Carbon nanotubes
D	: Dilatant
EDX	: Energy dispersive x-ray spectroscopy
EO	: Engine oil
EP	: Extreme pressure
FMs	: Friction modifiers
FWHM	: Full width at half maximum
GNP	: Graphene nanoplatelets
ICDD	: International centre for diffraction data
FHC	: Fluorinated hydrocarbon
KOH	: Potassium hydroxide
KI	: Potassium iodide
m	: Consistency index
MO	: Mineral Oil
MTPS	: Modified transient plane source
MWCNT	: Multiwalled carbon nanotubes
N	: Newtonian
n	: Power law index
NO	: Natural oil
OdW	: Ostwald–de Waele
PAG	: Poly alkylene glycol

PAO	:	Poly alpha olefin
PEG	:	Poly ethylene glycol
PFPE	:	Perfluoro polyether
PLGA	:	Poly (lactic-co-glycolic acid)
PMA	:	Poly alkyl methacrylate
PMMA	:	Poly (methyl methacrylate)
PP	:	Pseudo plastic
PPD	:	Pour point depressants
PS	:	Poly styrene
PSS	:	Poly styrene sulfonate
PTFE	:	Poly tetrafluoro ethylene
PVA	:	Poly vinyl alcohol
PVP	:	Poly vinyl pyrrolidone
R&CI	:	Rust and corrosion inhibitors
SAE	:	Society of automotive engineers
SEM	:	Scanning electron microscopy
SHC	:	Synthetic hydrocarbon
SiO	:	Silicone oil
SO	:	Synthetic oil
S.V.	:	Saponification value
SS	:	Stainless steel
VI	:	Viscosity index
WS2	:	Tungsten disulfide
TCP	:	Tricresylphosphate
WoS	:	Web of Science
XRD	:	X-ray diffraction
ZDP	:	Zinc dithiophosphate
ZDDP	:	Zinc dialkyldithiophosphate

# **Synopsis**

Of the thesis entitled

## **Nano-additives to improve the Flow and Thermal Properties of Different Oils**

Submitted to

**THE MAHARAJA SAYAJIRAO UNIVERSITY OF BARODA**

For the Degree of

**Doctor of Philosophy**

In

**Applied Chemistry**

By:

**Vishal Sureshkumar Vora**

Under the Supervision of

**Dr. Rakesh K. Sharma**



**Applied Chemistry Department  
Faculty of Technology and Engineering  
The Maharaja Sayajirao University of Baroda,  
Vadodara-390001, Gujarat, India**

**February -2024**

## Nano-additives to improve the flow and thermal properties of different oils

Oils, specifically industrial oils (IOs) play a crucial role as essential fluids employed across diverse applications in various industries[1]. These oils are formulated to meet the specific requirements of different machinery and equipment, providing necessary lubrication, protection, and performance enhancement[2,3]. From heavy-duty manufacturing to automotive applications, IOs play a critical role in ensuring the smooth operation of industrial manufacturing[4]. These oils are used as lubricants in the manufacturing industry for a variety of equipment, such as presses, pumps, and machine tools. They help to reduce friction and wear, thereby improving the longevity and performance of machinery[5]. The use of IOs also helps to minimize downtime, maintenance costs, and energy consumption in manufacturing operations, thereby increasing productivity and profitability. Engine oils, transmission fluids, and hydraulic fluids are also examples of IOs used in automotive applications. These oils help to protect engine parts from wear and tear, reduce friction, and ensure the smooth operation of various components in the vehicle. Not only that, industrial oils are used in construction applications like heavy equipment, cranes, and hydraulic systems. These oils are specifically designed to provide high levels of lubrication and protection in extreme operating conditions, such as high temperatures and heavy loads[6].

In addition to the above applications, IOs are also used in other industries, such as the food and beverage industry, pharmaceuticals, and electronics manufacturing. In the food and beverage industry, industrial oils are used for lubrication and corrosion protection in food processing and packaging equipment. In the pharmaceutical industry, they are utilized for smoothing of pharmaceutical processing equipment. In the electronics manufacturing industry, IOs are used for cooling and lubrication of cutting and drilling machines used in printed circuit board manufacturing[7,8].

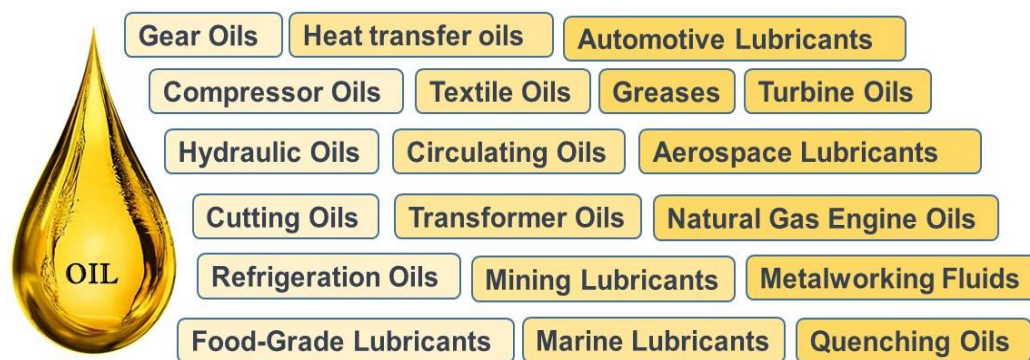


**Figure 1:** Types of IOs based on various applications[9]

Overall, the application of IOs is diverse and essential in various industries (Figure 1). These oils provide critical lubrication and protection for machinery and equipment, thereby ensuring the smooth and efficient operation of industrial processes and therefore, the demand for more specialized IOs with specific properties is very much increasing, and research and development in this area will play a critical role in it [4].

The sources of industrial oils are diverse, ranging from traditional vegetable and animal oils to modern synthetic and biofuel alternatives.

**Table 1:** Sources of IOs [10]

No.	Source Type	Examples
1	Vegetable oils	Olive oil, Sunflower oil, Soybean oil, Castor oil, Palm oil
2	Animal oils	Lard, Tallow, Fish oil, Cod liver oil
3	Mineral oils	Mineral oil, Petrolatum
4	Essential oils	Lavender oil, Peppermint oil, Tea tree oil
5	Synthetic oils	Synthetic motor oils, PAO oils, PEG oils
6	Fish oils	Cod liver oil, Salmon oil
7	Biofuels	Biodiesel, Algal oil
8	Fruit oils	Avocado oil, Mango seed oil, Passion fruit oil
9	Nut oils	Almond oil, Walnut oil, Hazelnut oil
10	Seed oils	Flaxseed oil, Sesame oil, Pumpkin seed oil
11	Herb oils	Basil oil, Rosemary oil, Thyme oil
12	Fungi oils	Mushroom oil

Vegetable oils, extracted from plant sources like seeds and fruits, include widely used varieties such as soybean and palm oil. Animal oils, derived from fats and tissues, find applications in various industrial sectors. Mineral oils, a product of petroleum refining, contribute significantly to industrial lubrication. Essential oils are known for their aromatic and therapeutic properties, offer very distinct applications. The emergence of synthetic oils and biofuels represents advancements in engineering oils tailored to specific industrial needs. Table 1 shows the diverse sources contributing to the formation of IOs [1, 3].

**Nano-additives**, also known as nanomaterial additives, are substances that consist of nanoscale particles or structures and are added to various materials to impart specific properties or enhance their performance. Nano-additives typically have at least one dimension at the nanometer scale, which is in the range of 1 to 100 nm. Nanoparticles, nanotubes, nanofibers, and nanoclays are commonly used as nano-additives. These additives play a crucial role in various industrial applications due to their unique properties and the

ability to enhance the performance of materials and products. When nano-additives are dispersed evenly in a base fluid like water, oils, or ethylene glycol, they create nanofluids. Nanofluids, a cutting-edge class of fluids, have gained significant popularity in research due to their unique properties and transformative potential. The nanoparticles confer exceptional thermal and rheological properties on the nanofluid, enhancing its heat transfer efficiency and flow characteristics. This heightened performance is attributed to the nanoparticles' large surface area, which facilitates improved thermal conductivity and fluid stability [9].

The use of nanofluids can significantly reduce engine wear and increase fuel efficiency. The nanoparticles form a protective layer on the engine surfaces, reducing friction and minimizing wear [11]. Additionally, the increased thermal stability of the oil prevents the formation of deposits and sludge, reducing the risk of engine damage. In hydraulic fluids, nano-additives can improve the lubricant's ability to withstand high-pressure and high-temperature conditions. The nanoparticles improve the fluid's shear strength, preventing it from breaking down under extreme conditions[12]. Similarly, in transmission fluids, the use of nano-additives can improve the fluid's ability to withstand high temperatures and pressures, reducing wear and extending the life of the transmission system [13]. Overall, the use of nano-additives in different oils as nanofluid has significant potential to enhance their performance properties and extend the life of mechanical systems. Researchers are exploring their applications in areas such as heat exchangers, electronics cooling, and automotive systems to address challenges related to thermal management and energy efficiency. The versatility and promising performance of nanofluids have propelled them to the forefront of scientific investigation and practical implementation[14].

The present research aims to study the performance characteristics of different oils by focusing on flow properties through rheology studies and thermal properties, i.e., thermal conductivity, in the presence of nano-additives. The approach involves the synthesis and evaluation of various nanofluids, wherein nano-additives are dispersed within base oils. The investigation mainly focuses on understanding the effects of specific nano-additives, namely alumina, zinc oxide, graphene nanoplatelets, and multiwalled carbon nanotubes, when introduced into distinctive base oils like castor oil and synthetic engine oil. Notably, castor oil, a non-edible fatty oil with a unique hydroxyl group structure, serves as a distinctive base fluid for synthesizing castor oil-based nanofluids. Recognizing its distinct properties, such as lubricative qualities, dielectric functionality, and heat transfer potential, castor oil proves to be an intriguing candidate for nanofluid development. In parallel, India's expansive two-wheeler automotive market underscores the critical role of engine oil, elevating the

significance of synthetic oils. Notably, 10W-30 synthetic engine oil emerges as a standout choice due to its remarkable versatility, delivering optimal performance across a diverse temperature range. This synthetic oil's inherent compatibility with nanoparticle dispersion is the driving force behind its selection for nanofluid research.

The study employs sophisticated characterization techniques, such as scanning electron microscopy (SEM), X-ray diffraction (XRD), and energy dispersive X-ray spectroscopy (EDX), to analyze the structural and chemical composition of the developed nano-additives. The hydrothermal method was employed to synthesize metal oxide based nano-additives. The probe-sonication method was used in the nanofluid development process to make sure that the nano-additives were evenly distributed in the base oils. A rheometer was used to measure the rheological properties of the synthesized nanofluids, and a thermal conductivity meter was used to measure their thermal conductivity. These analyses provide insights into the impact of nano-additives on the flow and thermal properties of the oils, which contribute valuable data to the broader understanding of IO applications.

In order to meet all the objectives of the present work, the contents of the thesis are summarized into seven chapters.

## **Chapter 1: General Introduction**

The present chapter covers the introduction of industrial oils (IOs) and their role in various applications. The chapter mainly focuses on two types of lubricating oils, such as castor oil (COs) and engine oil (EOs), for nanofluid synthesis. Various nano-additives and their potency in industrial applications have been described. The relevant research outputs in the area of the present work have been provided.

## **Chapter 2: Materials and Methods**

This chapter discusses the use of two different base oils for the synthesis of nanofluids: castor oil (COs) and engine oil (EOs). The complete procedure for extracting non-edible castor oil from oil-bearing seeds is explained. The physical and chemical characteristics of the extracted non-edible COs are provided and examined in detail. These characteristics include the saponification value, acid value, iodine value, specific gravity, hydroxyl number, and chemical composition. Simultaneously, the commercially available synthetic engine oil (EOs) of 10W-30 grade undergoes comprehensive evaluations for viscosity, pour point, flash point, and specific gravity. Furthermore, methodologies for rheological analysis and thermal conductivity analysis are briefly described to provide insights into the flow behavior and thermal properties of the fluids under investigation.

Moreover, rheometer and thermal conductivity meter instruments working principle explained in depth.

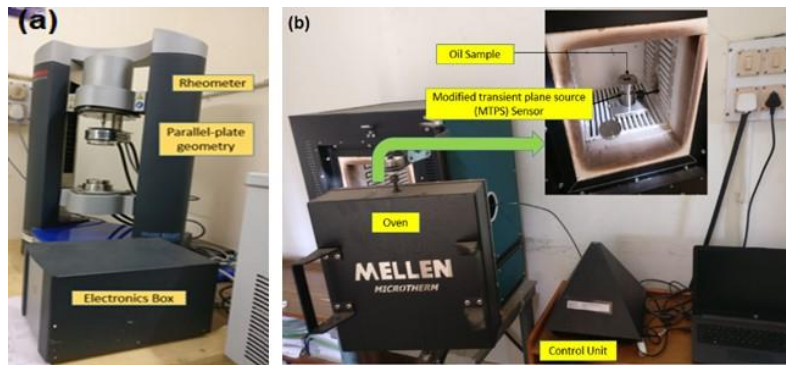


**Figure 2:** (a) Rotational rheometer (HAAKE MARS, Thermo scientific) and (b) Thermal conductivity analyzer (Trident, C-Therm Technologies) by using modified transient plane source (MTPS) technique

### Chapter 3: Nano-additives for development of Castor oil and Engine oil-based Nanofluids

For the development of COs and EOs based nanofluids, four different types of nano-additives have been chosen. Two important nano-additives Graphene nanoplatelets (GNP) and Multiwalled carbon nanotubes (MWCNT) were procured from Sigma-Aldrich (USA). The metal oxide based nano-additives: Alumina ( $\text{Al}_2\text{O}_3$ ) and Zinc oxide (ZnO), were typically synthesized through hydrothermal method. In a typical ZnO nano-additive hydrothermal synthesis, 10 mL of zinc nitrate  $\text{Zn}(\text{NO}_3)_2 \cdot 6\text{H}_2\text{O}$  (0.1 M) solution and 10 mL NaOH aqueous solution were vigorous stirring for 30min, and the slurry solutions were poured into Teflon lined autoclaves and hydrothermally heated at  $180^\circ\text{C}$  for 24 hours. The yield was washed with water then followed by ethanol, centrifuged and dried in an oven at overnight. Similarly,  $\text{Al}_2\text{O}_3$  nano-additives were synthesized using aluminum nitrate  $\text{Al}(\text{NO}_3)_3 \cdot 9\text{H}_2\text{O}$  as starting material and followed the procedure of ZnO nanoparticles.

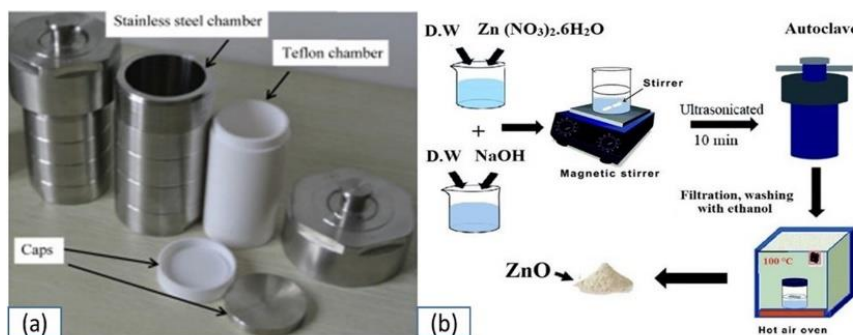


**Figure 3:**(a)Hydrothermal PTFE reactor with SS container, (b) Hydrothermal method for ZnO nano-additive synthesis

Here, the synthesized and purchased nano-additives were characterized by sophisticated characterization techniques, such as Scanning Electron Microscopy (SEM), X-ray Diffraction (XRD), and Energy Dispersive X-ray Spectroscopy (EDX), to analyze the structural and chemical composition of the developed nano-additives. Crystallite size less than 100 nm for all additives suggested the nanocrystalline nature and considered as nano-additives. The results of this chapter demonstrate that the developed additives can be used as nano-additives for the nano-fluid preparation to improve flow and thermal properties of base fluids.

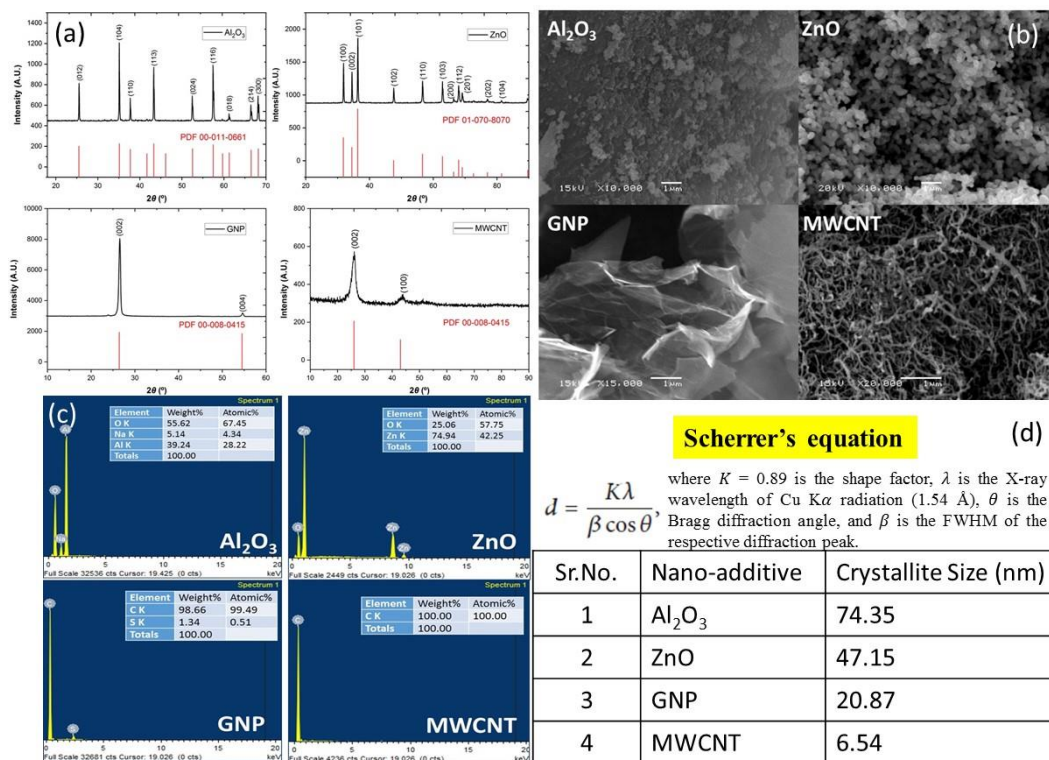


**Figure 4:**(a) X-ray Diffraction (XRD), (b) Scanning Electron Microscopy (SEM), (c) Energy Dispersive X-ray Spectroscopy (EDX) and (d) Crystallite Size determination using Scherrer's equation of developed nano-additives: Al<sub>2</sub>O<sub>3</sub>, ZnO, GNP and MWCNT.

## Chapter 4: Castor oil-based nanofluids containing Al<sub>2</sub>O<sub>3</sub>, ZnO, GNP and MWCNT nano-additives

Following CO-based nanofluids prepared by dispersing nano-additives.

1. CO-based nanofluid containing ZnO nano-additives
2. CO-based nanofluid containing Al<sub>2</sub>O<sub>3</sub> nano-additives
3. CO-based nanofluid containing GNP nano-additives
4. CO-based nanofluid containing MWCNT nano-additives

The nanofluid samples were prepared by adding nano-additives powder into pure CO by a double-step procedure. Homogeneous CO-based nanofluids were obtained by using a high-power ultra-sonication probe having a 500-watt output power and a 20 kHz frequency power supply.

In this chapter, a systematic exploration was undertaken to elucidate the rheological attributes of both base CO and CO-based nanofluids, encompassing CO/Al<sub>2</sub>O<sub>3</sub>, CO/ZnO, CO/GNP, and CO/MWCNT nanoformulations. The study explored dynamic viscosity under varying nano-additive concentrations (0.05, 0.1, 0.2, 0.5 weight %), shear rates, and temperatures. The primary focus on comprehended the impact of nano-additive weight percentage and temperature on the dynamic viscosity and thermal conductivity of all COs nanofluids, with potential applications as lubricating oils. To ascertain the flow behavior, whether it adheres to Newtonian or non-Newtonian flow, the Ostwald-de-Waele (OdW) model was employed using Equation (2):

$$\tau = m \cdot \gamma^n \dots\dots\dots (2)$$

Where  $\tau$  is shear stress,  $\gamma$  is shear rate,  $m$  is the consistency index, and  $n$  is the power law index. Power law curve fitting was applied to the shear stress against shear rate curve to determine the values of  $m$  and  $n$ . As showed in figure 6, results revealed non-linear viscosity trends at lower shear rates, linear behavior at higher shear rates, and a slight shear-thinning effect with increased GNP nano-additive concentration. Similarly, comprehensive flow behavior analyses were conducted for all other nanofluids, elucidating their distinct rheological characteristics. The study underscored the enhanced thermal conductivity of CO/GNP nanofluids compared to pure CO and other CO-based nanofluids, emphasizing their potential in improving heat transfer performance.

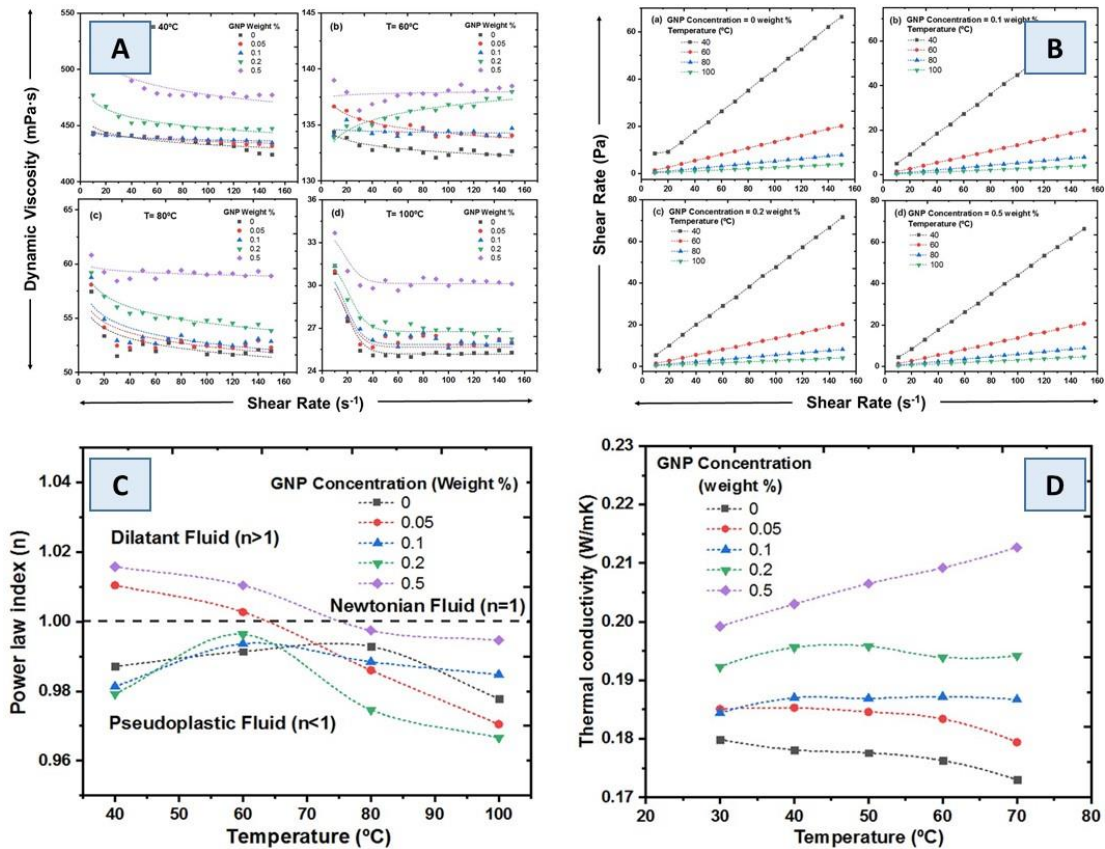


**Figure 5:**(A) Effect of shear rate on dynamic viscosity of CO/GNP nanofluids at different mass fraction, (B) Shear stress against shear rate at various temperature for CO/GNP nanofluids (C) Power law index for different solid mass fractions and temperature for CO/GNP nanofluids, (D) Thermal conductivity of CO/GNP nanofluids

## Chapter 5: Engine oil-based nanofluids containing Al<sub>2</sub>O<sub>3</sub>, ZnO, GNP and MWCNT nano-additives

Following EO-based nanofluids prepared by dispersing nano-additives.

1. EO-based nanofluid containing ZnO nano-additives
2. EO-based nanofluid containing Al<sub>2</sub>O<sub>3</sub> nano-additives
3. EO-based nanofluid containing GNP nano-additives
4. EO-based nanofluid containing MWCNT nano-additives

The nanofluid samples were prepared by adding nano-additives powder into EO of synthetic grade (10W-30) by a double-step procedure. Homogeneous EO-based nanofluids were obtained by using a high-power ultra-sonication probe having a 500-watt output power and a 20 kHz frequency power supply.

A systematic study was done in parallel to find out more about the flow properties of 10W-30 grade synthetic EO and its nanofluid counterparts, including EO/Al<sub>2</sub>O<sub>3</sub>, EO/ZnO, EO/GNP, and EO/MWCNT compounds. The investigation focused on dynamic viscosity under varied nano-additive concentrations (0.05, 0.1, 0.2, 0.5 weight %), shear rates, and temperatures, with a primary emphasis on comprehending the influence of nano-additive weight percentage and temperature on the dynamic viscosity and thermal conductivity of all EO-based nanofluids, offering potential applications in lubricating systems. Employing the Ostwald-de-Waele (OdW) model with Equation (1), where  $\tau$  represents shear stress,  $\dot{\gamma}$  is shear rate,  $m$  is the consistency index, and  $n$  is the power law index, enabled the determination of  $m$  and  $n$  values through power law curve fitting. In the same way, a full study of the flow behavior of all the other nanofluids was carried out, which showed how their unique rheological properties work. The study highlighted the augmented thermal conductivity of EO/GNP nanofluids compared to pure EO and other EO nanofluids, accentuating their potential for enhancing heat transfer performance in diverse applications.

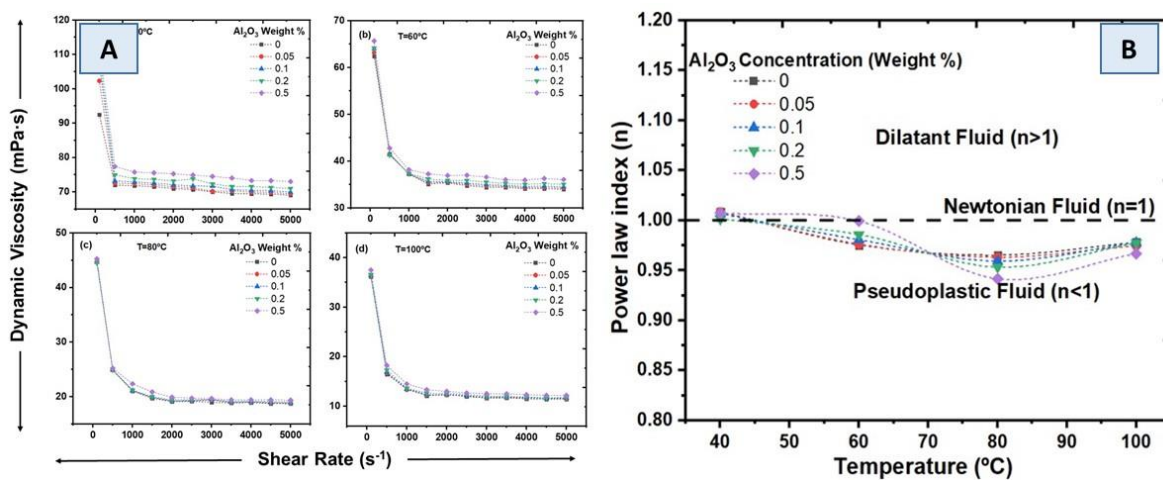


**Figure 6:**(A) Effect of shear rate on dynamic viscosity of EO/Al<sub>2</sub>O<sub>3</sub> nanofluids at different mass fraction, (B) Power law index for different solid mass fractions and temperature for EO/Al<sub>2</sub>O<sub>3</sub> nanofluids

## Chapter 6: Summary and Conclusions

The thesis ends with a summary of all the reported work and general conclusions drawn from the investigations.

## References:

1. Kajdas, C., A. Karpińska, and A. Kulczycki, Industrial Lubricants, in Chemistry and Technology of Lubricants, R.M. Mortier, M.F. Fox, and S.T. Orszulik, Editors. 2010, Springer Netherlands: Dordrecht. p. 239-292.
2. Boyde, S., Green lubricants. Environmental benefits and impacts of lubrication. Green Chemistry, 2002. 4(4): p. 293-307.
3. Tung, S.C. and M.L. McMillan, Automotive tribology overview of current advances and challenges for the future. Tribology International, 2004. 37(7): p. 517-536.
4. Nagendramma, P. and S. Kaul, Development of ecofriendly/biodegradable lubricants: An overview. Renewable and Sustainable Energy Reviews, 2012. 16(1): p. 764-774.
5. Grützmacher, P.G., et al., Multi-scale surface patterning – an approach to control friction and lubricant migration in lubricated systems. Industrial Lubrication and Tribology, 2019. 71(8): p. 1007-1016.
6. Katiyar, J.K., et al., Introduction of Automotive Tribology, in Automotive Tribology, J.K. Katiyar, et al., Editors. 2019, Springer Singapore: Singapore. p. 3-13.
7. Subhan, M.A., K.P. Choudhury, and N.J.N. Neogi, Advances with molecular nanomaterials in industrial manufacturing applications. 2021. 1(2): p. 75-97.
8. Mang, T. and A. Gosalia, Lubricants and Their Market, in Lubricants and Lubrication. 2017. p. 1-10.
9. Tonk, R., The science and technology of using nano-materials in engine oil as a lubricant additives. Materials Today: Proceedings, 2021. 37: p. 3475-3479.
10. Gerbig, Y., et al., Suitability of vegetable oils as industrial lubricants. Journal of Synthetic Lubrication, 2004. 21(3): p. 177-191.
11. Shahnazar, S., S. Bagheri, and S.B. Abd Hamid, Enhancing lubricant properties by nanoparticle additives. International Journal of Hydrogen Energy, 2016. 41(4): p. 3153-3170.
12. Ali, M.K.A., et al., Reducing frictional power losses and improving the scuffing resistance in automotive engines using hybrid nanomaterials as nano-lubricant additives. Wear, 2016. 364-365: p. 270-281.
13. Smith, S.R., et al., Application of aluminium oxide nanoparticles to enhance rheological and filtration properties of water based muds at HPHT conditions. Colloids and Surfaces A: Physicochemical and Engineering Aspects, 2018. 537: p. 361-371.
14. Vasishth, A., P. Kuchhal, and G. Anand, Study of Rheological Properties of Industrial Lubricants. Conference Papers in Science, 2014. 2014: p. 324615.

## List of the Research Publication

1. Investigation of Rheological and Thermal Conductivity Properties of Castor Oil Nanofluids Containing Graphene Nanoplatelets. International Journal of Thermophysics, 44(10), 155. Vishal Vora, Rakesh Sharma, D.P. Bharambe (2023). DOI: <https://doi.org/10.1007/s10765-023-03264-5>

## List of the Papers presented in the conferences/ Seminars/ Workshops

1. Oral presentation: Assessment of rheological behaviour and thermal conductivity of nonedible castor oil for possible lubrication applications, Vishal Vora, Rakesh Sharma, D.P. Bharambe, National conference on “Modern Trends in Chemistry”, 6th March 2022, organized by: Chemistry department & IQAC, RR Mehta College of Science and CC Mehta College of Commerce, Palanpur, Gujarat.
2. Poster Presentation: Investigation of Rheological and Thermal Conductivity Properties of Castor Oil Nanofluids Containing Graphene Nanoplatelets. Vishal Vora, Rakesh Sharma, D.P. Bharambe. International Seminar on Advanced Materials and Applications ISAMA 2022, The Maharaja Sayajirao University of Baroda, Vadodara, India, July 18, 2022

**Signature of Candidate**

**(Vishal Sureshkumar Vora)**

Endorsement of Supervisor;  
Synopsis is approved by me

**Dr.Rakesh K. Sharma**  
**Research Guide**

**Head**  
**Applied Chemistry Department**

**Dean**  
**Faculty of Technology and Engineering**